Journal of Photochemistry and Photobiology A: Chemistry 211 (2010) 135–142

Contents lists available at ScienceDirect

Journal of Photochemistry and Photobiology A: Chemistry

journal homepage: www.elsevier.com/locate/jphotochem

Synthesis and photoluminescence properties of four rhenium(I) complexes based on diimine ligands with oxadiazole/carbazole moiety

Jing Wu[a], Hong-Yan Li[a], Ling-Chen Kang[a], Dong-Ping Li[a], Huan-Rong Li[b], Xin-Hui Zhou[a], Yan Sui[a], You-Xuan Zheng[a,*], Jing-Lin Zuo[a], Xiao-Zeng You[a]

[a] State Key Laboratory of Coordination Chemistry, Nanjing National Laboratory of Microstructures, School of Chemistry and Chemical Engineering, Nanjing University, 22 Hankou Road, Nanjing 210093, PR China
[b] School of Chemical Engineering, Hebei University of Technology, Tianjin 300130, PR China

ARTICLE INFO

Article history:
Received 11 November 2009
Received in revised form 22 January 2010
Accepted 12 February 2010
Available online 21 February 2010

Keywords:
Carrier-transporting moieties
Oxadiazole
Carbazole
Diimine ligands
Rhenium(I) complexes

ABSTRACT

By introducing two carrier-transporting moieties (oxadiazole and carbazole) into two diimine ligands (2-(2-pyridine)-benzimidazole and 2,2′-dipyridylamine), respectively, four novel ligands (**L1–L4**) and their corresponding rhenium(I) complexes (**1–4**) have been synthesized and characterized by elemental analysis, ^{1}H NMR and IR spectra. Their photophysical properties, thermal analysis, along with the X-ray crystal structure analysis of **L4** and corresponding complex **4** are also described. In absorption spectra, the 2-(2-pyridine)-benzimidazole containing complexes **1**, **2** show the intraligand charge-transfer ($\pi \rightarrow \pi^*$ (L)) bands and metal-to-ligand charge-transfer $d\pi(Re) \rightarrow \pi^*$ MLCT bands, while the 2,2′-dipyridylamine containing complexes **3**, **4** only show the $\pi \rightarrow \pi^*$ bands. In the excitation spectra, all the complexes show strong MLCT bands. After excitation of $\pi \rightarrow \pi^*$ or MLCT bands, all the four Re(I) complexes exhibit broad bands around 550–560 nm due to the Re(I)-based ^{3}MLCT emission. The two complexes **1** (with oxadiazole moiety) and **2** (with carbazole moiety) show the photoluminescence quantum efficiency of 2.0% and 7.5% in solid state, respectively, indicating that the carbazole unit is the better chromophore to enhance the luminescence efficiency of diimine Re(I) complexes than the oxadiazole moiety.

1. Introduction

Since Forrest et al. [1] reported that electrophosphorescent materials could harvest both singlet and triplet excitons and endowed organic light-emitting devices (OLEDs) with a potential internal quantum efficiency of 100%, the electrophosphorescence of heavy metal complexes has been studied extensively [2,3]. Due to the distinguished qualities that Re(I) complexes possess such as photophysical, photochemical, excited state redox properties and with the aim of further exploring novel phosphorescent materials, more and more researchers pay considerable attention to this field [3–14].

However, most of the previously reported phosphorescent Re(I) complexes used in the OLEDs have the disadvantage of the saturation of emission sites causes the triplet–triplet annihilation, which leads to low efficiency at high current density [15–17]. There are two strategies available to manipulate original Re(I) complexes and to overcome the shortcoming mentioned above: (i) the synthesis of novel diimine ligands with different ligand-field are applied in molecular design [3,16,18,19] to adjust the molecular orbital energy levels in the Re(I) complexes which are related to the photochemical, photophysical and electrochemical events, because the spectroscopic and redox behavior of the Re(I) complexes are ligand dependent and can be tuned by varying the identity of their chelate ligands and (ii) the addition of functional groups with electro-donating or -accepting properties into diimine ligands [17,20–25] is efficient in improving the capability of OLEDs using the Re(I) complexes as the light-emitting layer and avoiding the triplet–triplet annihilation because of the steric hindrance effect.

In this article, according to these two methods, we designed four novel Re(I) complexes employing 2-(2-pyridine)-benzimidazole and 2,2′-dipyridylamine as the original diimine ligands and involving oxadiazole and carbazole moieties which own superior carrier-transporting ability. So, four ligands of 1-(4-5′-phenyl-1,3,4-oxadiazolylphenyl)-2-pyridinylbenzoimidazole (**L1**), 1-(4-carbazolylphenyl)-2-pyridinylbenzimidazole (**L2**), N-(4-5′-phenyl-1,3,4-oxadiazolyl-phenyl)-2,2′-dipyridylamine (**L3**), N-(4-carbazolylphenyl)-2,2′-dipyridylamine (**L4**) and their corresponding Re(I) complexes (**1–4**) have been synthesized successfully. In order to investigate the potential application in the OLEDs of the complexes, their optical and thermal stability are measured and discussed.

* Corresponding author. Tel.: +86 25 83596775; fax: +86 25 83314502.
E-mail address: yxzheng@nju.edu.cn (Y.-X. Zheng).

1010-6030/$ – see front matter © 2010 Elsevier B.V. All rights reserved.
doi:10.1016/j.jphotochem.2010.02.010

2. Experimental

2.1. Materials and instruments

Carbazole was purchased from Yuan Hang Reagent Company (China). 1,4-Dibromobenzene, 2-(4-bromophenyl)-5-phenyl-1,3,4-oxadiazole, benzoyl hydrazine, 2-(2-pyridyl)benzimidazole (**Pybm**), 2,2′-dipyridylamine (**Dpya**), 1,3-dimethyl-3,4,5,6-terahydro-2(1H)-pyrimidinone (DMPU) and rhenium pentacarbonyl chloride were brought from Acros, Aldrich and Alfa Companies. The IR spectra were taken on a Vector22 Bruker spectrophotometer (400–4000 cm^{-1}) with KBr pellets. NMR spectra were measured on a Bruker AM 500 spectrometer. Mass spectra were determined with an Autoflex ^{II}TM instrument for MALDI-TOF-MS or on a Varian MAT 311A instrument for ESI-MS. Elemental analyses for C, H, and N were performed on a PerkinElmer 240C analyzer. Absorption spectra were measured on a UV-3100 spectrophotometer. Photoluminescence measurements were carried out on Hitachi F4600 luminescence spectrophotometer equipped with a xenon arc lamp. The photoluminescence lifetime was measured with an Edinburgh Instruments FLS920P fluorescence spectrometer and obtained from time-resolved luminescence experiments at the MLCT excitation and maximal emission wavelengths. The quantum yield was determined using an integrating sphere (150 mm diameter, $BaSO_4$ coating) from Edinburgh Instruments according to the reported procedure [26]. The spectra were corrected for variations in the output of the excitation source and for variations in the detector response. The quantum yield can be defined as the integrated intensity of the luminescence signal divided by the integrated intensity of the absorption signal. Only the intense emission bands of the Re(I) complexes around 550 nm was measured by the integrating sphere being excited at the MLCT bands, but this intensity value was corrected by taking into account the relative intensity of the other transitions (as determined from the steady-state luminescence spectrum). In this way, an intensity value that corresponds to the total luminescence output was obtained. The absorption intensity was calculated by subtracting the integrated intensity of the light source with the sample in the integrating sphere from the integrated intensity of the light source with a blank sample in the integrating sphere.

The crystals of **L4** and **4** suitable for single-crystal X-ray analysis were obtained by slow evaporation of dichloromethane-hexane solution. The data were collected on a Bruker Smart Apex CCD diffractometer equipped with graphitemonochromated Mo Kα (λ = 0.71073 Å) radiation using a ω–2θ scan mode at 293 K. The highly redundant data sets were reduced using SAINT and absorption corrections were applied using SADABS supplied by Bruker. The structures were solved by direct methods and refined by full-matrix least-squares methods on F^2 using SHELXTL-97. Thermogravimetrical and differential thermal analysis (TGA–DTA) was performed in N_2 atmosphere with a flow rate of 100 mL/min on a simultaneous SDT 2960 thermal analyzer from 20 to 750 °C, with a ramp rate of 10 °C/min.

2.2. Synthesis

The chemical structures of the materials used in this work and the synthetic routes were depicted in Scheme 1. The ligand precursors 2-(4-bromophenyl)-5-phenyl-1,3,4-oxadiazole (**a**) and 1-carbazolyl-4-bromobenzene (**b**) were synthesized as described in literature [27,28]. The four ligands of 1-(4-5′-phenyl-1,3,4-oxadiazolylphenyl)-2-pyridinylbenzoimidazole (**L1**), 1-(4-carbazolyl-phenyl)-2-pyridinylbenzimidazole (**L2**), N-(4-5′-phenyl-1,3,4-oxadiazolyl-phenyl)-2,2′-dipyridylamine (**L3**), N-(4-carbazolylphenyl)-2,2′-dipyridylamine (**L4**) and the corresponding Re(I) complexes of **1–4** were prepared according to modified procedure [27,29]. Complexes $Re(CO)_3Cl$(Pybm) (**5**) and $Re(CO)_3Cl$(Dpya) (**6**) were also prepared as reference materials by the same method.

Synthesis of 2-(4-bromophenyl)-5-phenyl-1,3,4-oxadiazole **(a)**: 4-Bromobenzoyl chloride (21.95 g, 0.1 mol) was added dropwise to a solution of benzoyl hydrazine (13.62 g, 0.1 mol) and triethylamine (10.10 g, 0.1 mol) in chloroform (150 mL) at room temperature (RT). The resulting mixture was stirred for 1 h and then filtered. The collected solid was washed with water and ethanol to give the product N′-benzoyl-4-bromobenzohydrazide (30.32 g, yield 95%). A mixture of N′-benzoyl-4-bromobenzo-hydrazide (20.00 g) and $POCl_3$ (250 mL) in a 500 mL flask was refluxed under nitrogen for 5 h. The excessive $POCl_3$ was then distilled out, and the residue was poured into water. The crude solid state product was collected by filtration and purified by recrystallization from chloroform/hexane to give **a** as white needlelike crystals (16.04 g, yield: 85%). M.p.: 164–168 °C. IR (KBr, cm^{-1}): 3060, 1600, 1546, 1474, 1073, 728, 689. ^{1}H NMR ($CDCl_3$, 500 MHz): δ 8.159 (d, 2H, J = 7 Hz), 8.040 (d, 2H, J = 9 Hz), 7.710 (d, 2H, J = 8.5 Hz), 7.570 (m, 3H). MS (ESI): m/z 301.08 $[M]^+$. Anal. Calcd. for $C_{14}H_9N_2OBr$: C, 55.84; H, 3.01; N, 9.30. Found: C, 55.87; H, 3.11; N, 9.27.

Synthesis of 1-carbazolyl-4-bromobenzene **(b)**: Similar methods (see Scheme 1) are used to prepare **b**, **L1**, **L2**, **L3** and **L4**. A mixture of carbazole (16.72 g, 0.1 mol), 1,4-dibromobenzene (23.59 g, 0.1 mol), CuI (1.90 g, 0.01 mol), 18-Crown-6 (0.88 g, 0.0033 mol), K_2CO_3 (27.67 g, 0.2 mol) and DMPU (3 mL) was put into reactor, then keep it heating at 170 °C for 13 h under nitrogen. After cooling to room temperature, the mixture was quenched with 1N HCl, the precipitate was filtered and washed with $NH_3{\cdot}H_2O$ and water. The brown solid was purified with column chromatography using hexane as eluant (10.95 g, yield: 34%). M.p.: 152–154 °C. IR (KBr, cm^{-1}): 3056, 1496, 1452, 1230, 751. ^{1}H NMR ($CDCl_3$, 500 MHz): δ 8.175 (d, 2H, J = 7 Hz), 7.757 (d, 2H, J = 8.5 Hz), 7.495 (d, 2H, J = 8.5 Hz), 7.431 (t, 2H, J = 7 Hz), 7.411 (d, 2H, J = 9 Hz), 7.342 (t, 2H, J = 7.5 Hz). MS (MALDI-TOF): m/z 321.035 $[M]^+$. Anal. Calcd. for $C_{18}H_{12}NBr$: C, 67.10; H, 3.75; N, 4.35. Found: C, 66.93; H, 3.71; N, 4.31.

Synthesis of 1-(4-5′-phenyl-1,3,4-oxadiazolylphenyl)-2-pyridinylbenzoimidazole **(L1)**: The procedure is similar to that of compound **b** with the materials of **a** (3.01 g, 0.01 mol) and **Pybm** (1.95 g, 0.01 mol) at the temperature of 230 °C (2.50 g, yield: 60%). M.p.: 186–189 °C. IR (KBr, cm^{-1}): 3050, 1606, 1500, 1442, 1385, 773, 755, 741, 708, 691. ^{1}H NMR ($CDCl_3$, 500 MHz): δ 8.380 (d, 3H, J = 7.5 Hz), 8.200 (d, 2H, J = 7.5 Hz), 7.987 (t, 1H, J = 7.5 Hz), 7.603–7.577 (m, 7H), 7.525 (t, 2H, J = 7.5 Hz), 7.405 (t, 1H, J = 6 Hz), 7.321(d, 1H, J = 8.5 Hz). MS (MALDI-TOF): m/z 416.232 $[M]^+$. Anal. Calcd. for $C_{26}H_{17}N_5O$: C, 75.17; H, 4.12; N, 16.86. Found: C, 75.11; H, 4.21; N, 16.81.

Synthesis of 1-(4-carbazolylphenyl)-2-pyridinylbenzimidazole **(L2)**: The procedure is similar to that of compound **b** with the materials of **b** (3.22 g, 0.01 mol) and **Pybm** (1.95 g, 0.01 mol) at the temperature of 230 °C (2.93 g, yield: 67%). M.p.: 225–228 °C. IR (KBr, cm^{-1}): 3044, 1728, 1593, 1514, 1446, 740. ^{1}H NMR ($CDCl_3$, 500 MHz): δ 8.489 (d, 2H, J = 4.5 Hz), 8.203 (d, 2H, J = 7.5 Hz), 8.074 (d, 1H, J = 8 Hz), 7.906 (t, 1H, J = 7.5 Hz), 7.762 (d, 2H, J = 8.5 Hz), 7.614 (d, 2H, J = 9 Hz), 7.550 (d, 2H, J = 7.5 Hz), 7.502 (t, 3H, J = 7 Hz), 7.472 (m, 2H), 7.357 (t, 3H, J = 7 Hz). MS (MALDI-TOF): m/z 437.130 $[M]^+$. Anal. Calcd. for $C_{30}H_{20}N_4$: C, 82.55; H, 4.62; N, 12.84. Found: C, 82.54; H, 4.69; N, 12.83.

Synthesis of N-(4-5′-phenyl-1,3,4-oxadiazolylphenyl)-2,2′-dipyridylamine **(L3)**: The procedure is similar to that of compound **b** with the materials of **a** (3.01 g, 0.01 mol) and **Dpya** (1.71 g, 0.01 mol) at the temperature of 180 °C (2.31 g, yield: 59%). M.p.: 136–140 °C. IR (KBr, cm^{-1}): 2994, 1588, 1496, 1467, 1332, 772, 740, 708, 685. ^{1}H NMR ($CDCl_3$, 500 MHz): δ 8.573 (m, 2H), 8.217 (d, 2H, J = 8.5 Hz), 8.149 (d, 2H, J = 8 Hz), 7.755 (t, 2H, J = 7.5 Hz), 7.578 (m, 3H), 7.392 (d, 2H, J = 8.5 Hz), 7.158 (m, 2H), 7.021 (d, 2H, J = 8 Hz). MS (MALDI-TOF): m/z 392.169 $[M]^+$. Anal. Calcd. for

$C_{24}H_{17}N_5O$: C, 73.64; H, 4.38; N, 17.89. Found: C, 73.67; H, 4.31; N, 17.97.

Synthesis of N-(4-carbazolylphenyl)-2,2′-dipyridylamine **(L4)**: The procedure is similar to that of compound **b** with the materials of **b** (3.22 g, 0.01 mol) and **Dpya** (1.71 g, 0.01 mol) at the temperature of 180 °C (3.71 g, yield: 90%). M.p.: >290 °C. IR (KBr, cm^{-1}): 3040, 1582, 1512, 1458, 1442, 1320, 754. ^1H NMR ($CDCl_3$, 500 MHz): δ 8.595 (m, 2H), 8.174 (d, 2H, J = 7.5 Hz), 7.753 (m, 2H), 7.695 (d, 2H, J = 7 Hz), 7.564 (d, 2H, J = 8 Hz), 7.487 (m, 4H), 7.323 (t, 2H, J = 7 Hz), 7.122 (m, 2H), 7.063 (d, 2H, J = 8 Hz). MS (MALDI-TOF): m/z 412.234 $[M]^+$. Anal. Calcd. for $C_{28}H_{20}N_4$: C, 81.53; H, 4.89; N, 13.58. Found: C, 81.44; H, 4.83; N, 13.57.

Synthesis of **1**: **L1** (0.21 g, 0.5 mmol) and $Re(CO)_5Cl$ (0.18 g, 0.5 mmol) were refluxed in 30 mL of anhydrous toluene for 6 h. After the mixture was cooled to RT, the solvent was distilled out. The resulting yellow solid was purified by silica gel column chromatography with dichloromethane and hexane (v/v = 2:1, 5% in volume Et_3N was added) to get **1** (0.25 g, yield: 70%). M.p.: 230–232 °C. IR (KBr, cm^{-1}): 2924, 2020, 1904, 1880, 754. ^1H NMR ($CDCl_3$, 500 MHz): δ 9.206 (d, 1H, J = 5 Hz), 8.608 (d, 1H, J = 8 Hz), 8.535 (d, 1H, J = 9 Hz), 8.226 (t, 3H, J = 9.5 Hz), 7.808 (m, 3H), 7.638 (m, 4H), 7.559 (m, 2H), 7.215 (d, 1H, J = 8.5 Hz), 7.175 (d, 1H, J = 8.5 Hz). MS (MALDI-TOF): m/z 686.162 $[M-Cl]^+$. Anal. Calcd. for $C_{29}H_{17}N_5O_4ClRe$: C, 48.30; H, 2.38; N, 9.71. Found: C, 48.27; H, 2.37; N, 9.72.

Synthesis of **2**: The procedure is similar to that of **1** (0.26 g, yield: 70%). M.p.: >300 °C. IR (KBr, cm^{-1}): 2017, 1905 (b), 750. ^1H NMR ($CDCl_3$, 500 MHz): δ 9.227 (d, 1H, J = 6 Hz), 8.235 (t, 3H, J = 7 Hz), 8.046 (t, 2H, J = 7.5 Hz), 7.879 (m, 3H), 7.652 (m, 3H), 7.576 (m, 4H), 7.430 (t, 2H, J = 7.5 Hz), 7.322 (m, 2H). MS (MALDI-TOF): m/z 717.67 $[M-Cl]^+$. Anal. Calcd. for $C_{33}H_{20}N_4O_3ClRe$: C, 53.40; H, 2.72; N, 7.55. Found: C, 53.27; H, 2.87; N, 7.54.

Synthesis of **3**: The procedure is similar to that of **1** (0.28 g, yield: 79%). M.p.: 218–220 °C. IR (KBr, cm^{-1}): 2020, 1896 (b), 1433, 779, 732, 714. ^1H NMR ($CDCl_3$, 500 MHz): δ 9.104 (d, 2H, J = 7 Hz), 8.245 (d, 2H, J = 9 Hz), 8.152 (d, 2H, J = 8.5 Hz), 7.994 (t, 2H, J = 8 Hz), 7.597

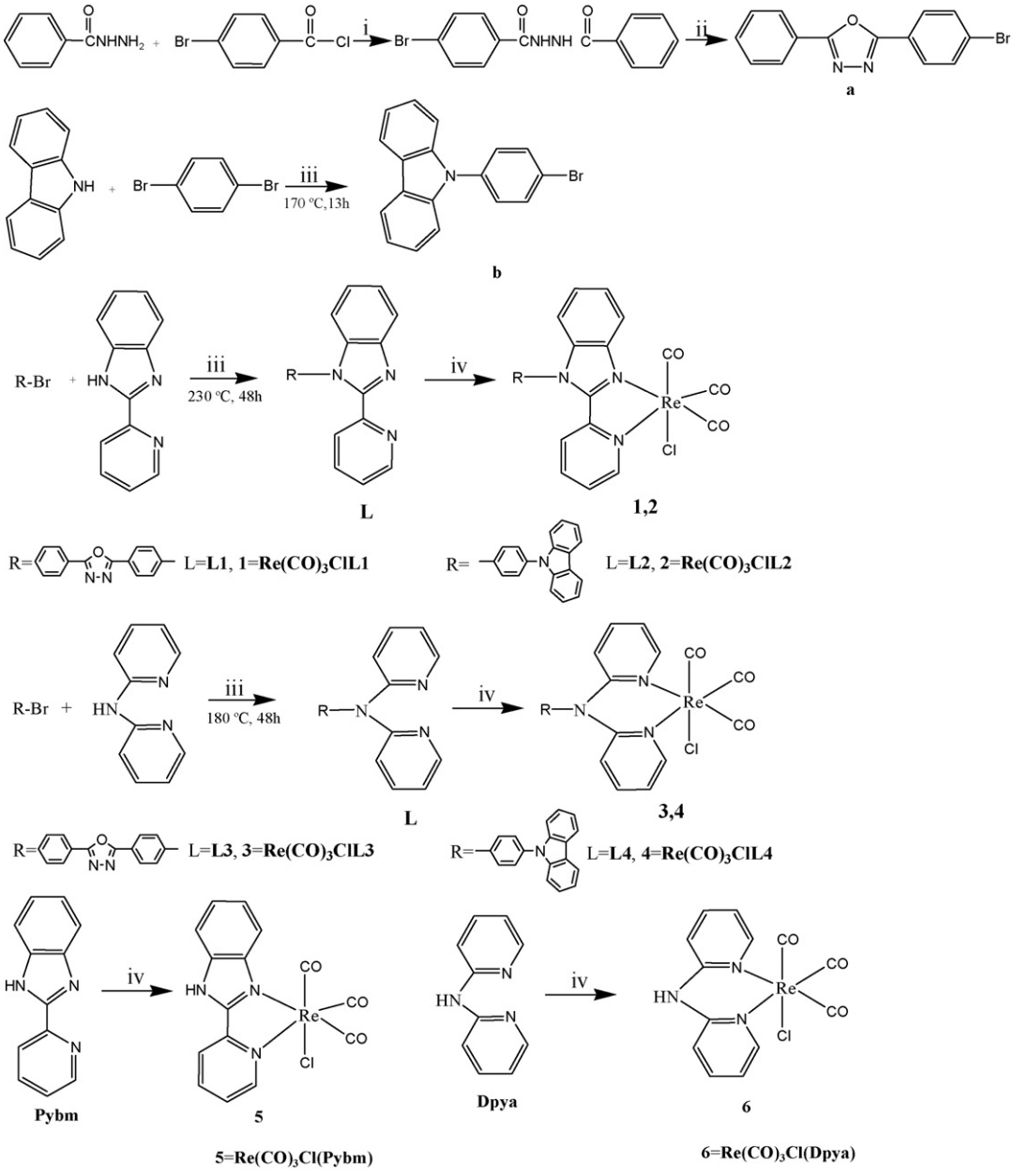

Scheme 1. Synthetic routes for **a**, **b**, **L1–L4** and **1–6**. (i) Et_3N, $CHCl_3$, RT; (ii) $POCl_3$, reflux; (iii) CuI, 18-Crown-6, K_2CO_3, DMPU, in reactor; (iv) $Re(CO)_5Cl$, toluene, reflux.

(m, 6H), 7.405 (m, 5H). MS (MALDI-TOF): m/z 662.125 $[M-Cl]^+$. Anal. Calcd. for $C_{27}H_{17}N_5O_4ClRe$: C, 46.52; H, 2.46; N, 10.05. Found: C, 46.47; H, 2.46; N, 10.01.

Synthesis of **4**: The procedure is similar to that of **1** (0.23 g, yield: 63%). M.p.: >290 °C. IR (KBr, cm^{-1}): 2018, 1909, 1889, 749. ^1H NMR ($CDCl_3$, 500 MHz): δ 9.048 (m, 2H), 8.209 (d, 2H, J = 7.5 Hz), 7.896 (m, 2H), 7.852 (d, 2H, J = 8.5 Hz), 7.800 (d, 2H, J = 8.5 Hz), 7.530–7.441 (m, 7H), 7.369 (t, 3H, J = 7 Hz). MS (MALDI-TOF): m/z 683.132 $[M-Cl]^+$. Anal. Calcd. for $C_{31}H_{20}N_4O_3ClRe$: C, 51.84; H, 2.81; N, 7.80. Found: C, 51.81; H, 2.84; N, 7.87.

3. Results and discussion

3.1. Crystallography

The crystallographic data for the **L4** and **4** support the structures of these compounds. The crystal data are presented in Table 1 and selected bond distances and angles for the compounds are listed in Table 2. With respect to the **L4** (Fig. 1), the length of the C(9)–N(2) bond connecting carbazole group and the benzene ring is 1.437(8) Å. The C(10)–N(2)–C(9) bond angle is 125.8(3)°. The bond C(6)–N(1) between the benzene ring and **Dpya** is 1.429(9) Å. The C(5)–N(1)–C(6) bond angle is 120.6(3)°. Carbazole group and the benzene ring are not coplanar with a dihedral angle of 49.19°.

An ORTEP diagram of **4** is also shown in Fig. 1. The coordination geometry at the Re atom is a distorted octahedron with the three carbonyl ligands arranged in a facial fashion. The distances of C(29), C(30) and C(31) to Re(1) are 1.88(1) Å averagely and the average Re–N bond length is 2.160(8) Å. All the bond distance data are in agreement with analogous Re(I) diimine complexes [16,30]. The C–Re–C bond angels are in the range of 86.0(5)–89.7(4)°, which is close to 90°, the O–C–Re bond angels are close to 180° indicating that CO ligands are linearly coordinated, while the N–Re–N bond angle is 80.9(3)°, which is much less than 90°, this is possibly due to the steric requirement of the bidentate coordination of the **L4** ligand.

3.2. Photophysical properties

The UV–vis absorption spectra of the **L1–L4** and corresponding Re(I) complexes **1–4** are exhibited in Fig. 2. For all of the Re(I) complexes, the dominant absorption bands in the 230–350 nm region are assigned to the intraligand charge-transfer ($\pi \rightarrow \pi^*$ (L)) transition by comparing with their corresponding free ligands, this rule is common in most Re(I) complexes [31]. We can see the absorptions at longer wavelength for **1** and **2** extend to visible region from 350 to 500 nm with weaker intensities. The metal-to-ligand charge-transfer $d\pi$ (Re) $\rightarrow \pi^*$ (N–N) MLCT is tentatively accounted for these bands [32,10,33]. By comparing the bands of the four Re(I) complexes, we can also find that the charge-transfer $d\pi$ (Re) $\rightarrow \pi^*$ (N–N) bands of **1** and **2** are more evident than the later two complexes. For comparison, the UV–vis absorption spectra of two complexes **5** and **6** without functional moieties are also presented in Fig. 2. From Fig. 2a we can find that after adding carbazole/oxidazole moiety to **Pybm**, the higher-energy absorption peaks of derived Re-complexes shifted to longer wavelength. This phenomenon can be explained as follows: the structure of **Pybm** is rigid, the conjugated plate of derived ligands was enlarged, and the energy of LUMO becomes lower. While the structure of **Dpya** is flexible, the additional moieties have no evident influence on the conjugated plate, so the corresponding absorption peaks of **3**, **4** and **6** have no remarkable change (Fig. 2b).

Fig. 3 and Table 3 show photoluminescence properties of the **L1–L4** and **1–4** in solid state under ambient conditions. From Fig. 3a it can be found that the major excitation bands of ligands are similar in shape, belonging to the $\pi \rightarrow \pi^*$ transitions of carrier-transporting moieties and **Pybm/Dpya**. The excitation spectra of all the complexes (Fig. 3b) measured by monitoring the respective emission λ_{max} are also similar in shape to each other. The bands are centered at around 468 nm with weaker shoulders which are assigned to MLCT transitions as depicted above. However, the excitation spectrum of **4** is unusual. The stronger band sites at shorter wavelength about 400 nm, in opposite, the intensity of longer wavelength excitation is weaker. By comparing the excitation spectra of free ligands with their corresponding complexes, it is worthy to note that the excitation spectra of the complexes gain red shift. The emission spectra of complexes centralize at around 550–560 nm upon being excited with the

Table 1
Crystallographic data for **L4** and **4**.

	L4	**4**
Formula	$C_{28}H_{20}N_4$	$C_{31}H_{20}ClN_4O_3Re$
FW	412.49	718.16
T (K)	291(2)	291(2)
Wavelength (Å)	0.71073	0.71073
Crystal system	Orthorhombic	Triclinic
Space group	*Fdd2*	*P*-1
a (Å)	15.309(3)	10.5233(16)
b (Å)	14.380(3)	14.873(2)
c (Å)	19.508(5)	17.719(3)
α (°)	90.00	87.012(2)
β (°)	90.00	88.711(2)
γ (°)	90.00	79.754(2)
V (Å^3)	4294.6(17)	2725.1(7)
Z	1	4
ρ_{calcd} (g/cm^3)	1.276	1.750
μ (Mo Kα) (mm^{-1})	0.077	4.598
F(000)	1728	1400
Range of transm factors (°)	2.1–20.4	1.85–25.00
Reflns collected	5184	13908
Unique	1813	9487
Data/restraints/params	1813/1/148	9487/0/721
GOF on F^2	0.912	0.780
R_1^a, wR_2^b [$I > 2\sigma(I)$]	0.0528, 0.1200	0.0526, 0.0979
R_1^a, wR_2^b (all data)	0.1054, 0.1563	0.1009, 0.1105
CCDC No.	736721	729550

$R_1^a = \Sigma||F_o| - |F_c||/\Sigma|F_o|$. $wR_2^b = [\Sigma w(F_o^2 - F_c^2)^2/\Sigma w(F_o^2)]^{1/2}$.

Table 2
Selected bond lengths (Å) and angles (°) for **L4** and **4**.

L4[a]		**4**	
C(4)–N(3)	1.331(6)	Re(1)–C(29)	1.87(1)
C(5)–N(3)	1.329(6)	Re(1)–C(30)	1.88(1)
C(5)–N(1)	1.406(6)	Re(1)–C(31)	1.89(1)
C(6)–N(1)	1.429(9)	Re(1)–N(3)	2.157(8)
C(9)–N(2)	1.437(8)	Re(1)–N(4)	2.163(8)
C(10)–N(2)	1.385(5)	Re(1)–Cl(1)	2.485(3)
N(3)–C(4)–C(3)	123.2(5)	C(29)–Re(1)–C(30)	89.7(4)
N(3)–C(5)–C(1)	121.6(5)	C(29)–Re(1)–C(31)	88.7(5)
N(3)–C(5)–N(1)	116.7(4)	C(30)–Re(1)–C(31)	86.0(5)
C(1)–C(5)–N(1)	121.7(5)	C(29)–Re(1)–N(3)	94.5(4)
C(7)–C(6)–N(1)	120.6(3)	C(30)–Re(1)–N(3)	174.8(4)
C(8)–C(9)–N(2)	119.4(3)	C(31)–Re(1)–N(3)	97.0(4)
N(2)–C(10)–C(15)	129.2(4)	C(29)–Re(1)–N(4)	92.3(4)
N(2)–C(10)–C(11)	109.2(4)	C(30)–Re(1)–N(4)	96.0(4)
C(5)–N(1)–C(5A)	118.9(6)	C(31)–Re(1)–N(4)	177.8(4)
C(5)–N(1)–C(6)	120.6(3)	N(3)–Re(1)–N(4)	80.9(3)
C(10)–N(2)–C(10A)	108.4(5)	C(29)–Re(1)–Cl(1)	177.8(3)
C(10)–N(2)–C(9)	125.8(3)	C(30)–Re(1)–Cl(1)	90.9(3)
C(5)–N(3)–C(4)	118.0(4)	C(31)–Re(1)–Cl(1)	93.5(3)
		N(3)–Re(1)–Cl(1)	84.7(2)
		N(4)–Re(1)–Cl(1)	85.4(2)
		O(1)–C(29)–Re(1)	173.6(10)
		O(2)–C(30)–Re(1)	176.7(11)
		O(3)–C(31)–Re(1)	175.4(11)

[a] Symmetry code: 7/4 + x, 9/4 − y, 3/4 + z.

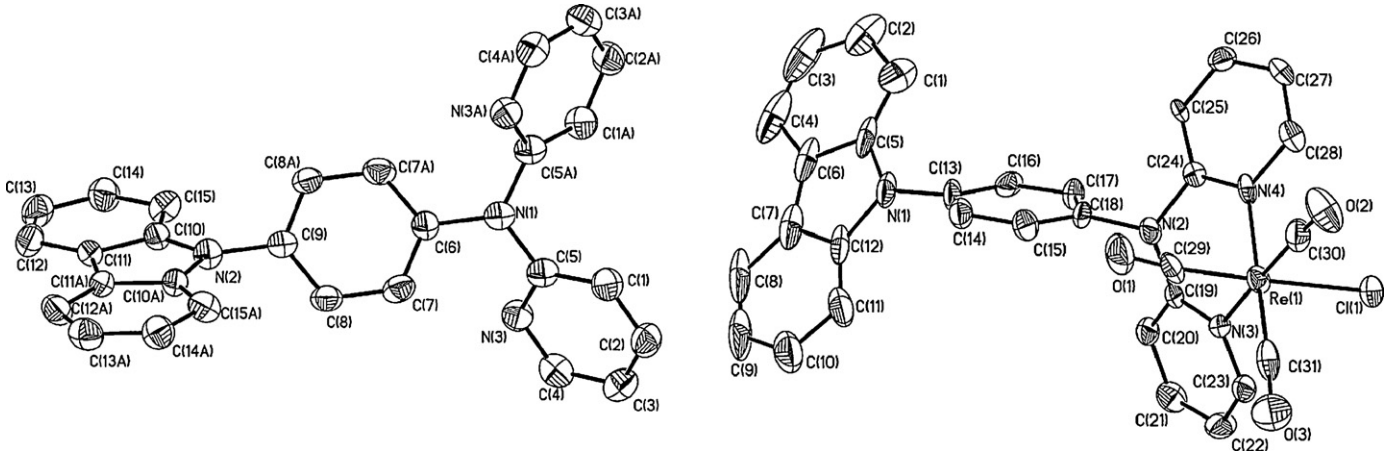

Fig. 1. ORTEP view of **L4** (symmetry code: $7/4+x$, $9/4-y$, $3/4+z$) and **4** with the atom-numbering scheme. Hydrogen atoms are omitted for clarity. Ellipsoids are drawn at the 30% probability level.

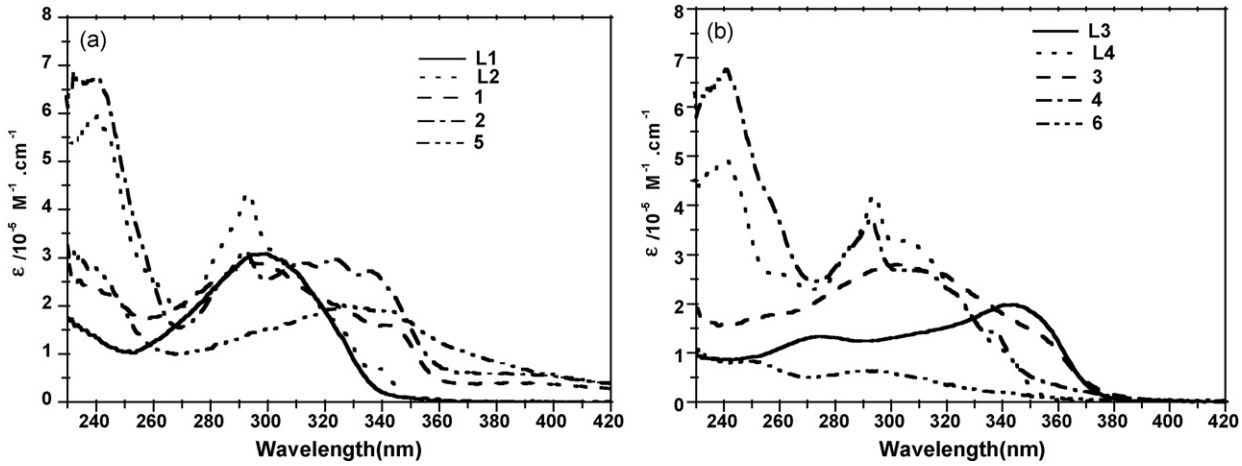

Fig. 2. UV–vis absorption of **L1–L4** and **1–6** in CH_2Cl_2 solution at room temperature.

maximum excitation peaks are characteristic of Re(I)-based MLCT emission frequently found in $Re(CO)_3ClL$ (L = polypyridine) complexes [32]. It also exhibits that the emission spectra of **1** and **2** are more intense than the later two complexes, this could be due to more rigid structure of **Pybm** type complexes compared with that of **Dypa** ones. Ward et al. [34] reported that the coordination ring of the ligand with Re(I) also can affect the luminescence. In the **Dypa** type complexes, coordination of the ligand at the Re(I) centre takes place with formation of a 6-membered chelate ring (see above), as opposed to a 5-membered one for **Pybm** type luminescent Re(I) complexes [35–39]. This is likely to result in a lower ligand-field strength for the present cases. As a consequence, lower-lying, thermally accessible d–d MC levels could provide an efficient non-radiative path for disposal of the excitation energy in the Re(I) complexes reported here. This behavior is well known for derivatives of $[Ru(bipy)_3]^{2+}$ in which the ligand-field strength around the metal is reduced by steric distortions [40–43] and has recently been demonstrated for a range of Re(I)-tricarbonyl-diimine complexes [44] although it should be noted that a range of other non-radiative decay pathways are in principle available [44,45].

The supposed nature of the emitting states is also supported by the corresponding radiative decays which lie in the microsecond timescale domain typical for MLCT and IL transitions. The luminescence decay curves of all the complexes were obtained

Table 3
The photoluminescence data of Re(I) complexes at room temperature in solid state.

Complex	Excitation	Emission		Lifetime (μs)[d]	
	λ, nm	λ_{max}, nm[a,b]	ϕ (%)[c]	τ_1	τ_2
1	373, 441, 494	565	2.0	1.48 (52.45%)	13.13 (47.55%)
2	370, 442, 490	562	7.5	1.67 (47.49%)	10.62 (52.51%)
3	380, 406, 438	432, 514, 547	[e]	1.48 (51.00%)	12.15 (49.00%)
4	400	426, 547, 595	[e]	1.46 (53.18%)	13.91 (46.82%)

[a] Emission maxima from not corrected spectra.
[b] Excited by the highest excitation peak.
[c] Obtained from time-resolved luminescence experiments at the MLCT excitation and maximal emission wavelengths.
[d] Be detected at the excitation wavelength is 468 nm, and the emission is monitored at their MLCT emission peaks around 550 nm in solid state.
[e] Not detected.

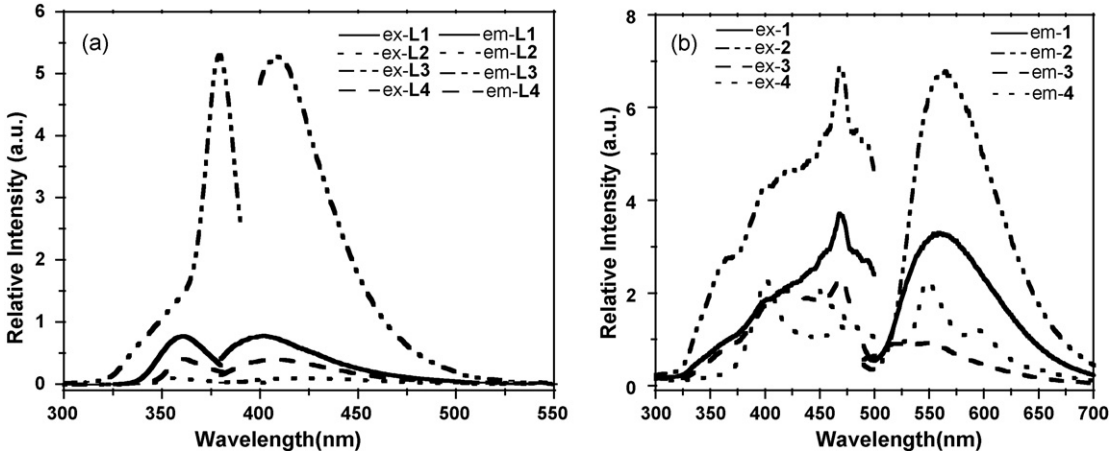

Fig. 3. (a) Excitation and emission spectra of **L1–L4** in solid state; (b) excitation and emission spectra of **1–4** in solid state. All the spectra were measured under ambient conditions.

from time-resolved luminescence experiments at the MLCT excitation and maximal emission wavelengths. As indicated in Fig. 4 and Table 3, the decay curves of all complexes measured in solid state are composed of two exponential decays with lifetimes of 1.32–1.67 μs (~50%) and 10.62–14.84 μs (~50%) [46–48]. The Re(I) carbonyl complexes that show multiexponential decay kinetics are known, confirming the existence of two light-emission excited states with comparable energies [46–48]. The long-lived component is thus assigned to the emission from the π–π* state and the shorter-lived component is assigned to the emission from the MLCT state. In general, if there is potential surface crossing from the higher ligand π–π* state to the lower MLCT state, one can expect, on the basis of the energy gap law, a shorter decay lifetime of the π–π* state than the lower MLCT state [46–48]. We

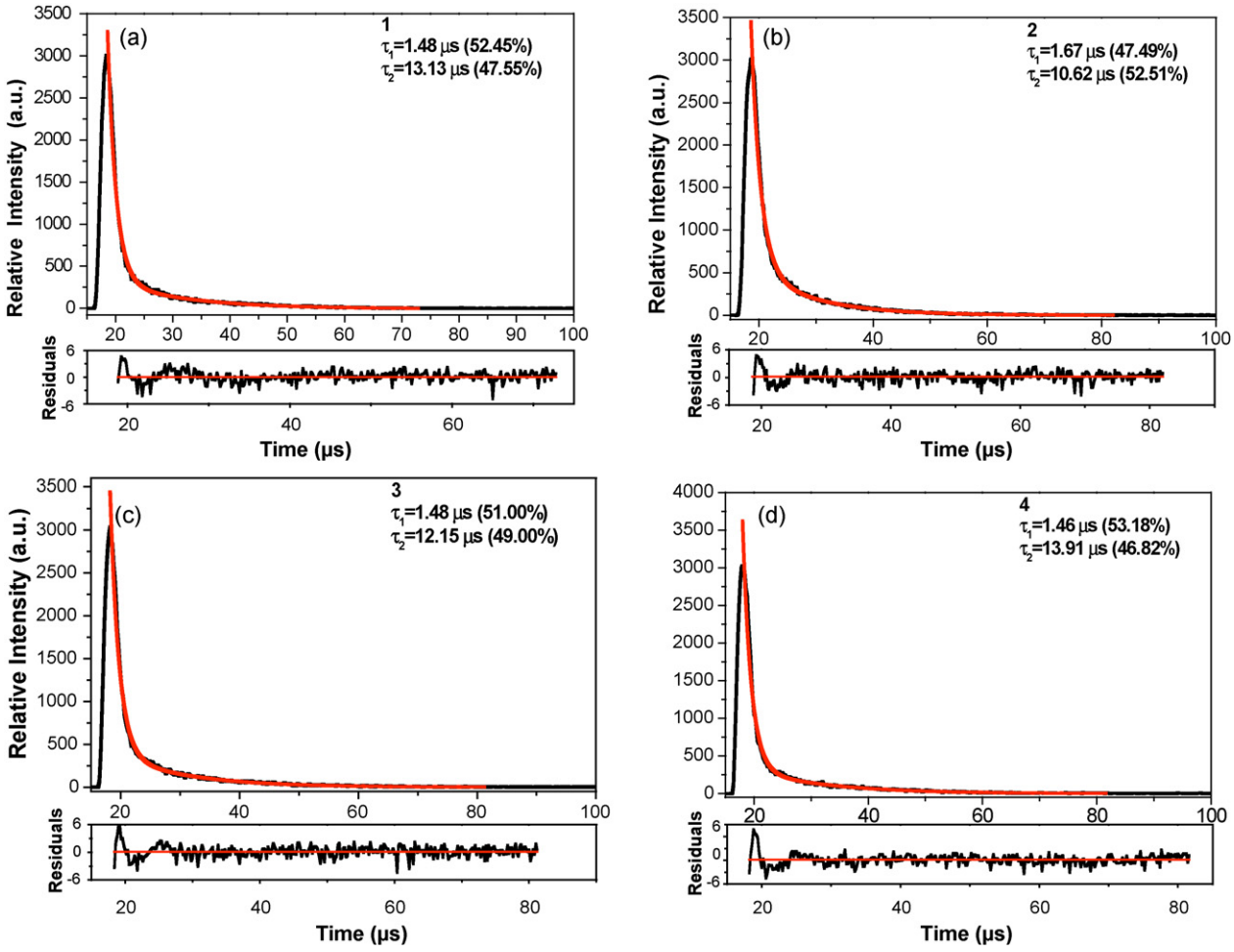

Fig. 4. Photoluminescence lifetime decay measurement of **1–4** in solid state at room temperature. The excitation wavelength is 468 nm, and the emission is monitored at their MLCT emission peaks around 550 nm.

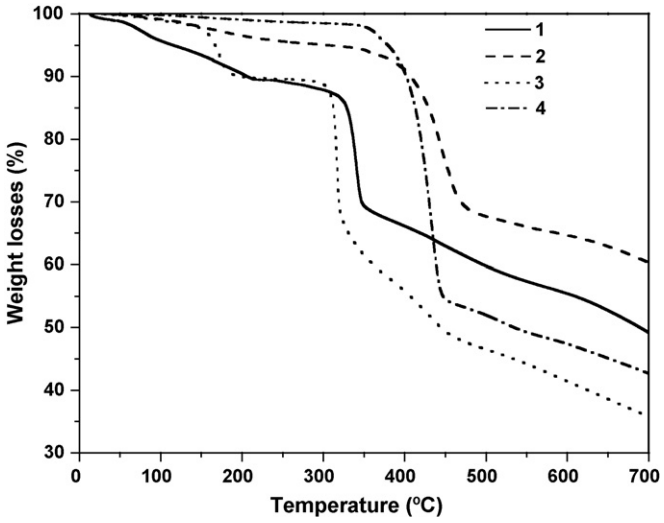

Fig. 5. TGA traces for the **1–4**.

further probed the photophysical properties of **1** and **2** by measuring their photoluminescence quantum efficiency in solid state using an integrating sphere (150 mm diameter, $BaSO_4$ coating) from Edinburgh Instruments according to the reported procedure [26], the data are 2.0% and 7.5%, respectively. The data are agree with the luminescence intensity sequence in Fig. 3 indicating the carbazole unit is the better chromophore to enhance the luminescence efficiency of diimine Re(I) complexes than oxadiazole moiety in our cases. This function of carbazole unit has been reported in literature [49,50].

3.3. Thermal analysis

In order to investigate the stable characteristics of all the four Re(I) complexes, TGA was performed on them in a N_2 atmosphere, and the traces are presented in Fig. 5. Complex **1** began to lose weight when the temperature reached at 322 °C, the loss of the chlorine anion and carbonyl groups can account for this. **2**, **3** and **4** show the similar thermal characteristics as **1** in a N_2 atmosphere: they began to decompose for the same reason at 374, 302 and 356 °C, respectively. **3** shows another weight loss at 149 °C possibly due to that the sample is not dry enough, it lost water at this temperature. The weight loss at the temperature higher than 400 °C is probably caused by the unassisted thermolysis of ligands or simply its sublimation.

4. Conclusion

We have synthesized four novel ligands and their corresponding Re(I) complexes with oxadiazole or carbazole moiety successfully. All the Re(I) complexes exhibit better photoluminescent properties in solid state than those without functional moieties. It also exhibits that the emission spectra of **1** and **2** are more intense than **3** and **4**, this could be due to more rigid structure of **Pybm** type complexes compared with that of **Dypa** ones. Besides that, the carbazole containing complex **2** shows higher quantum efficiency (7.5%) in solid state than the oxadiazole containing complex **1** (2.0%) indicating the carbazole unit is the better chromophore to enhance the luminescence properties of diimine Re(I) complexes than oxadiazole moiety.

Acknowledgments

This work was supported by the National Natural Science Foundation of China (Grant 20701019, 20971067 and 20721002), the Natural Science Foundation of Jiangsu Province (Grant BK2008257), the Major State Basic Research Development Program (2006CB806104 and 2007CB925103) and the Research Fund for the Doctoral Program of Higher Education (Grant 20070284053).

References

[1] M.A. Baldo, D.F. O'Brien, Y. You, A. Shoustikov, S. Sibley, M.E. Thompson, S.R. Forrest, Highly efficient phosphorescent emission from organic electroluminescent devices, Nature 395 (1998) 151–154.
[2] H.J. Bolink, L. Cappelli, E. Coronado, M. Grätzel, E. Ortí, R.D. Costa, P.M. Viruela, M.K. Nazeeruddin, Stable single-layer light-emitting electrochemical cell using 4,7-diphenyl-1,10-phenanthroline-bis(2-phenylpyridine)iridium(III) hexafluorophosphate, J. Am. Chem. Soc. 128 (2006) 14786–14787.
[3] Y. Li, Y. Wang, Y. Zhang, Y. Wu, J. Shen, Carbonyl polypyridyl Re(I) complexes as organic electroluminescent materials, Synth. Met. 99 (1999) 257–260.
[4] K.K.W. Lo, K.H.K. Tsang, N. Zhu, Luminescent tricarbonylrhenium(I) polypyridine estradiol conjugates: synthesis, crystal structure, and photophysical, electrochemical, and protein-binding properties, Organometallics 25 (2006) 3220–3227.
[5] M. Busby, P. Matousek, M. Towrie, I.P. Clark, M. Motevalli, F. Hartl, A. Vlc̆ek Jr., Rhenium-to-benzoylpyridine and rhenium-to-bipyridine MLCT excited states of fac-[Re(Cl)(4-benzoylpyridine)(2)(CO)(3)] and fac-[Re(4-benzoylpyridine)(CO)(3)(bpy)](+): a time-resolved spectroscopic and spectroelectrochemical study, Inorg. Chem. 43 (2004) 4523–4530.
[6] L. Wei, J.W. Babich, W. Ouellette, J. Zubieta, Developing the $\{M(CO)_3\}^+$ core for fluorescence applications: rhenium tricarbonyl core complexes with benzimidazole, quinoline, and tryptophan derivatives, Inorg. Chem. 45 (2006) 3057–3066.
[7] H. Tsubaki, A. Sekine, Y. Ohashi, K. Koike, H. Takeda, O. Ishitani, Control of photochemical, photophysical, electrochemical, and photocatalytic properties of rhenium(I) complexes using intramolecular weak interactions between ligands, J. Am. Chem. Soc. 127 (2005) 15544–15555.
[8] N. Marti, B. Spingler, F. Breher, R. Schibli, Comparative studies of substitution reactions of rhenium(I) dicarbonyl-nitrosyl and tricarbonyl complexes in aqueous media, Inorg. Chem. 44 (2005) 6082–6091.
[9] A. Gabrielsson, F. Hartl, H. Zhang, J.R. Lindsay Smith, M. Towrie, A. Vlček Jr., R.N. Perutz, Ultrafast charge separation in a photoreactive rhenium-appended porphyrin assembly monitored by picosecond transient infrared spectroscopy, J. Am. Chem. Soc. 128 (2006) 4253–4266.
[10] B.J. Coe, N.R.M. Curati, E.C. Fitzgerald, S.J. Coles, P.N. Horton, M.E. Light, M.B. Hursthouse, Syntheses and properties of bimetallic chromophore-quencher assemblies containing ruthenium(II) and rhenium(I) centers, Organometallics 26 (2007) 2318–2329.
[11] D.L. Reger, R.P. Watson, M.D. Smith, P.J. Pellechia, Bitopic phenylene-linked bis(pyrazolyl)methane ligands: preparation and supramolecular structures of hetero- and homobimetallic complexes incorporating organoplatinum(II) and tricarbonylrhenium(I) centers, Organometallics 24 (2005) 1544–1555.
[12] S.C.F. Lam, V.W.W. Yam, K.M.C. Wong, E.C.C. Cheng, N. Zhu, Synthesis and characterization of luminescent rhenium(I)–platinum(II) polypyridine bichromophoric alkynyl-bridged molecular rods, Organometallics 24 (2005) 4298–4305.
[13] A. Albertino, C. Garino, S. Ghiani, R. Gobetto, C. Nervi, L. Salassa, E. Rosenberg, A. Sharmin, G. Viscardi, R. Buscaino, G. Croce, M. Milanesio, Photophysical properties and computational investigations of tricarbonylrhenium(I) [2-(4-methylpyridin-2-yl)benzo[d]-X-azole]L and tricarbonylrhenium(I)[2-(benzo[d]-X-azol-2-yl)-4-methylquinoline]L derivatives (X = N-CH_3, O, or S; L = Cl^-, pyridine), J. Organomet. Chem. 692 (2007) 1377–1391.
[14] V.W.W. Yam, W.Y. Lo, C.H. Lam, W.K.M. Fung, K.M.C. Wong, V.C.Y. Lau, N. Zhu, Synthesis and luminescence behavior of mixed-metal rhenium(I)–copper(I) and –silver(I) alkynyl complexes, Coord. Chem. Rev. 245 (2003) 39–47.
[15] V.W.W. Yam, B. Li, Y. Yang, B.W.K. Chu, K.M.C. Wong, K.K. Cheung, Preparation, photo-luminescence and electro-luminescence behavior of Langmuir–Blodgett Films of bipyridylrhenium(I) surfactant complexes, Eur. J. Inorg. Chem. 25 (2003) 4035–4042.
[16] K. Wang, L. Huang, L. Gao, L. Jin, C. Huang, Synthesis, crystal structure, and photoelectric properties of $Re(CO)_3ClL$ (L = 2-(1-ethylbenzimidazol-2-yl)pyridine), Inorg. Chem. 41 (2002) 3353–3358.
[17] B. Li, M. Li, Z. Hong, W. Li, T. Yu, H. Wei, Observation of red intraligand electrophosphorescence from a stilbene-containing Re(I) complex, Appl. Phys. Lett. 85 (2004) 4786–4788.
[18] F. Li, G. Cheng, Y. Zhao, J. Feng, S. Liu, M. Zhang, Y. Ma, J. Shen, White-electrophosphorescence devices based on rhenium complexes, Appl. Phys. Lett. 83 (2003) 4716–4718.
[19] G. David, P.J. Walsh, K.C. Gordon, Red electroluminescence from transparent PVK-dye films based on dipyrido[3,2-a:20,30-c]phenazine and $Re(CO)_3Cl$-dipyrido[3,2-a:20,30-c]phenazine dyes, Chem. Phys. Lett. 383 (2004) 292–296.

[20] C. Fu, M. Li, Z. Su, Z. Hong, W. Li, B. Li, Improved performance of electrophosphorescent devices based on $Re(CO)_3Cl$-dipyrido[3,2-a:2′,3′-c]phenazine, Appl. Phys. Lett. 88 (2006) 093507–093509.
[21] F. Li, M. Zhang, G. Cheng, J. Feng, Y. Zhao, Y. Ma, S. Liu, J. Shen, Highly efficient electrophosphorescence devices based on rhenium complexes, Appl. Phys. Lett. 84 (2004) 148–150.
[22] X. Gong, P.K. Ng, W.K. Chan, Trifunctional light-emitting molecules based on rhenium and ruthenium bipyridine complexes, Adv. Mater. 10 (1998) 1337–1340.
[23] Y. Li, Y. Liu, J. Guo, F. Wu, W. Tian, B. Li, Y. Wang, Photoluminescent and electroluminescent properties of phenol-pyridine beryllium and carbonyl polypyridyl Re(I) complexes codeposited films, Synth. Met. 118 (2001) 175–179.
[24] F. Li, M. Zhang, J. Feng, G. Cheng, Z. Wu, Y. Ma, S. Liu, Red electrophosphorescence devices based on rhenium complexes, Appl. Phys. Lett. 83 (2003) 365–367.
[25] W.K. Chan, P.K. Ng, X. Gong, S. Hou, Light-emitting multifunctional rhenium (I) and ruthenium (II) 2,2′-bipyridyl complexes with bipolar character, Appl. Phys. Lett. 75 (1999) 3920–3922.
[26] P. Lenaerts, K. Driesen, R. Van Deun, K. Binnemans, Covalent coupling of luminescent tris(2-thenoyltrifluoro acetonato)lanthanide(III) complexes on a merrifield resin, Chem. Mater. 17 (2005) 2148–2154.
[27] Q. Zhang, J.S. Chen, Y.X. Cheng, L.X. Wang, D.G. Ma, X.B. Jing, F.S. Wang, Novel hole-transporting materials based on 1,4-bis(carbazolyl)benzene for organic light-emitting devices, J. Mater. Chem. 14 (2004) 895–900.
[28] Z. Peng, Z. Bao, M.E. Galvin, Oxadiazole-containing polymers for light-emitting diodes, Adv. Mater. 10 (1998) 680–684.
[29] J.V. Caspar, T.J. Meyer, Application of the energy gap law to nonradiative, excited-state decay, J. Phys. Chem. 87 (1983) 952–957.
[30] T. Rajendran, B. Manimaran, F.Y. Lee, G.H. Lee, S.M. Peng, C.C. Wang, K.L. Lu, First light-emitting neutral molecular rectangles, Inorg. Chem. 39 (2000) 2016–2017.
[31] Z.J. Si, J. Li, B. Li, F.F. Zhao, S.Y. Liu, W.L. Li, Synthesis, structural characterization, and electrophosphorescent properties of rhenium(I) complexes containing carrier-transporting groups, Inorg. Chem. 46 (2007) 6155–6163.
[32] W. Liu, R. Wang, X.H. Zhou, J.L. Zuo, X.Z. You, Syntheses, structures, and properties of tricarbonyl rhenium(I) heteronuclear complexes with a new bridging ligand containing coupled bis(2-pyridyl) and 1,2-dithiolene units, Organometallics 27 (2008) 126–134.
[33] R. Kirgan, M. Simpson, C. Moore, J. Day, L. Bui, C. Tanner, D.P. Rillema, Synthesis, characterization, photophysical, and computational studies of rhenium(I) tricarbonyl complexes containing the derivatives of bipyrazine, Inorg. Chem. 46 (2007) 6464–6472.
[34] N.M. Shavaleev, A. Barbieri, Z. Bell, M.D. Ward, F. Barigelletti, New ligands in the 2,2′-dipyridylamine series and their Re(I) complexes; synthesis, structures and luminescence properties, New J. Chem. 28 (2004) 398–405.
[35] M.D. Ward, F. Barigelletti, Control of photoinduced energy transfer between metal-polypyridyl luminophores across rigid covalent, flexible covalent, or hydrogen-bonded bridges, Coord. Chem. Rev. 216–217 (2001) 127–154.
[36] S. Encinas, K.L. Bushell, S.M. Couchman, J.C. Jeffrey, M.D. Ward, L. Flamigni, F. Barigelletti, J. Chem. Soc., Dalton Trans. (2000) 1783–1792.
[37] W.M. Xue, N. Goswami, D.M. Eichhorn, P.L. Orizondo, D.P. Rillema, synthesis and luminescence properties of a nonsymmetrical ligand-bridged Re^{I}–Re^{I} chromophore, Inorg. Chem. 39 (2000) 4460–4467.
[38] K.A. Walters, K.D. Ley, C.S.P. Cavalaheiro, S.E. Miller, D. Gosztola, M.R. Wasielewski, A.P. Bussandri, H. van Willigen, K.S. Schanze, photophysics of π-conjugated metal–organic oligomers: aryleneethynylenes that contain the $(bpy)Re(CO)_3Cl$ chromophore, J. Am. Chem. Soc. 123 (2001) 8329–8342.
[39] V.W.W. Yam, K.M.C. Wong, S.H.F. Chong, V.C.Y. Lau, S.C.F. Lam, L.J. Zhang, K.K. Cheung, Synthesis, electrochemistry and structural characterization of luminescent rhenium(I) monoynyl complexes and their homo- and hetero-metallic binuclear complexes, J. Organomet. Chem. 670 (2003) 205–220.
[40] R.H. Fabian, D.M. Klassen, R.W. Sonntag, Synthesis and spectroscopic characterization of ruthenium and osmium complexes with sterically hindering ligands. 3. Tris complexes with methyl- and dimethyl-substituted 2,2′-bipyridine and 1,10-phenanthroline, Inorg. Chem. 19 (1980) 1977–1982.
[41] J.M. Kelly, C. Long, C.M. O'Connell, J.G. Vos, A.H.A. Tinnemenans, Preparation, spectroscopic characterization, and photochemical and electrochemical properties of some bis(2,2′-bipyridyl)ruthenium(II) and tetracarbonyltungsten(0) complexes of 6-p-tolyl-2,2′-bipyridyl and of 6-p-styryl-2,2′-bipyridyl and its copolymers, Inorg. Chem. 22 (1983) 2818–2824.
[42] E.C. Constable, M.J. Hannon, A.M.W. Cargill Thompson, D.A. Tocher, J.V. Walker, A principle for the assembly of novel mononuclear building blocks for supramolecular chemistry, Supramol. Chem. 2 (1993) 243–246.
[43] A.M. Barthram, M.D. Ward, A. Gessi, N. Armaroli, L. Flamigni, F. Barigelletti, Spectroscopic, luminescence and electrochemical studies on a pair of isomeric complexes $[(bipy)_2Ru(AB)PtCl_2][PF_6]_2$ and $[Cl_2Pt(AB)Ru(bipy)_2][PF_6]_2$, where AB is the bis-bipyridyl bridging ligand 2,2′:3′,2″:6″,2‴-quaterpyridine, New J. Chem. 22 (1998) 913–917.
[44] K. Koike, N. Okoshi, H. Hori, K. Takeuchi, O. Ishitani, H. Tsubaki, I.P. Clark, M.W. George, F.P.A. Johnson, J.J. Turner, Mechanism of the photochemical ligand substitution reactions of fac-$[Re(bpy)(CO)_3(PR_3)]^+$ complexes and the properties of their triplet ligand-field excited states, J. Am. Chem. Soc. 124 (2002) 11448–11455.
[45] L.A. Worl, R. Duesing, P. Chen, L.D. Ciana, T.J. Meyer, Photophysical properties of polypyridyl carbonyl complexes of rhenium(I), J. Chem. Soc., Dalton Trans. (1991) 849–858.
[46] J.R. Shaw, R.H. Schmehl, Photophysical properties of rhenium(I) diimine complexes: observation of room-temperature intraligand phosphorescence, J. Am. Chem. Soc. 113 (1991) 389–394.
[47] L. Wallace, D.P. Rillema, Photophysical properties of rhenium(I) tricarbonyl complexes containing alkyl- and aryl-substituted phenanthrolines as ligands, Inorg. Chem. 32 (1993) 3836–3843.
[48] D.R. Striplin, G.A. Crossby, Photophysical investigations of $rhenium(I)Cl(CO)_3$(phenanthroline) complexes, Coord. Chem. Rev. 211 (2001) 163–175.
[49] X.H. Li, J. Gui, H. Yang, W.J. Wu, F.Y. Li, H. Tian, C.H. Huang, A new carbazole-based phenanthrenyl ruthenium complex as sensitizer for a dye-sensitized solar cell, Inorg. Chim. Acta 361 (2008) 2835–2840.
[50] S.H. Fan, K.Z. Wang, W.C. Yang, A carbazole-containing difunctional Ru^{II} complex that functions as a pH-induced emission switch and an efficient sensitizer for solar cells, Eur. J. Inorg. Chem. (2009) 508–518.